QUENCHING PROCESS MODELING IN STEEL CYLINDERS USING A MULTI-PHASE CONSTITUTIVE MODEL

Wendell Porto Oliveira
Luís Felipe Guimarães de Souza
Pedro Manuel Calas Lopes Pacheco
CEFET/RJ - Department of Mechanical Engineering
20.271-110 - Rio de Janeiro - RJ - Brazil
E-Mail: wendellporto@uol.com.br,lfelipe@cefet-rj.br,calas@cefet-rj.br

Marcelo Amorim Savi
COPPE/UFRJ - Department of Mechanical Engineering
21.945-970 – Rio de Janeiro – RJ – Brazil
Cx. Postal 68.503
E-Mail: savi@ufrj.br

Abstract. *Quenching is a commonly used heat treatment for hardening of steels. The resulting microstructures, which could be formed from quenching, depend on cooling rate and on the chemical composition of steel. The internal stresses generated during quenching can produce warping and even cracking and, therefore, the prediction of such stresses is relevant. Phenomenological aspects of quenching involve couplings between three different physical processes, thermal, mechanical and phase transformation, and its description is unusually complex. This article is concerned with the modeling and simulation of quenching in steel cylinders using a constitutive model that includes seven phases (austenite, ferrite, cementite, pearlite, upper bainite, lower bainite and martensite microstructures). JMAK (Johnson, Mehl, Avrami and Kolmogorov) law describes kinetics of diffusional phase transformations, while non-diffusive transformations are described by Koistinen-Marburger law. A numerical procedure is developed based on operator split technique associated with an iterative numerical scheme in order to deal with the non-linearities in the formulation. Numerical simulations are carried out analyzing some aspects related to the cooling process. Results suggest that the proposed model is capable of capturing the main behavior observed in experimental data.*

Keywords. *Quenching, Phase Transformation, Thermo-mechanical Coupling, Modeling, Numerical Simulation.*

1. Introduction

Quenching is a heat treatment usually employed in industrial processes. It provides a mean to control mechanical properties of steels as toughness and hardness. The process consists of raising the steel temperature above a certain critical value, holding it at that temperature for a fixed time, and then rapidly cooling it in a suitable medium to room temperature. The resulting microstructures formed from quenching (ferrite, cementite, pearlite, upper bainite, lower bainite and martensite) depend on cooling rate and on chemical composition of the steel. The volume expansion associated with the formation of martensite combined with large temperature gradients and non-uniform cooling can promote high residual stresses in quenching steels. As these internal stresses can produce warping and even cracking of a steel body, the prediction of such stresses is an important task.

Phenomenological aspects of quenching involve couplings among different physical processes and its description is unusually complex. Basically, three couplings are essential: thermal, phase transformation and mechanical phenomena. Since the quenching problem involves different knowledge areas, several authors have addressed these three aspects separately. Sen *et al.* (2000) considers steel cylinders without phase transformations. Others focus on the modeling of the phase transformation phenomena (Denis *et al.*, 1992; Hömberg, 1996; Chen *et al.*, 1997, Çetinel *et al.*, 2000; Reti *et al.*, 2001). Several authors have proposed coupled models that are not generic and are usually applicable to simple geometries as cylinders (Inoue & Wang, 1985; Melander, 1985; Sjöström, 1985; Denis *et al.*, 1985, 1987, 1999; Denis, 1996; Fernandes *et al.*, 1985; Woodard, *et al.*, 1999; Gür & Tekkaya, 1996, 2001). There are complex aspects that are usually neglected in the analysis of quenching process. As an example, one could mention the heat generated during phase transformation which some authors treats by means of the latent heat associated with phase transformation (Inoue & Wang, 1985; Denis *et al.*, 1987, 1999; Sjöstrom, 1994; Woodward *et al.*, 1999). Meanwhile, other coupling terms in the energy equation related to other phenomena as plastic strain or hardening are not treated in literature and their analysis is an important topic to be investigated.

This article is concerned with the modeling and simulation of quenching in steel cylinders using a constitutive anisothermal model that includes seven phases (austenite, cementite, ferrite, pearlite, upper bainite, lower bainite and martensite microstructures). The kinetics of the diffusive transformations is described by *JMAK* (Johnson, Mehl, Avrami e Kolmogorov) law (Avrami, 1940; Cahn, 1956), while non-diffusive transformations is described by Koistinen-Marburger law (Koistinen & Marburger, 1959). The proposed model is based on a model formulated within the framework of continuum mechanics and the thermodynamics of irreversible processes considering two phases: austenite and martensite (Pacheco *et al.* 1997, 2001a,b; Silva *et al.*, 2002). The adopted approach is general and allows a direct extension to more complex situations. The model includes thermomechanical couplings in the energy equation associated with phase transformation, plasticity and hardening, allowing the investigation of the effects promoted by these coupling (Silva *et al.*, 2002). A numerical procedure is developed based on the operator split technique (Ortiz *et al.*, 1983) associated with an iterative numerical scheme in order to deal with non-linearities in the formulation. With this assumption, the coupled governing equations are solved from four non-coupled problems: thermal, phase transformation, thermoelastic and elastoplastic. The proposed general formulation is applied to progressive induction and through hardening of steel cylinders. Numerical results show that the proposed model is capable of capturing the main behavior observed on experimental data.

2. Phenomenological Aspects of Phase Transformation

In quenching process, a steel piece is heated and maintained at constant temperature until austenite is obtained. Afterwards, a cooling process promotes the transformation of austenite into up to seven different microstructures: ferrite, cementite, pearlite, upper bainite, lower bainite and martensite. In order to describe all these microstructures, one represents the volumetric fraction of each as a phase β_i (austenite $i = A$, ferrite $i = 1$, cementite $i = 2$, pearlite $i = 3$, upper bainite $i = 4$, lower bainite $i = 5$ and martensite $i = M$). All these phases may coexist, satisfying the following constraints: $\beta_A + \beta_1 + \beta_2 + \beta_3 + \beta_4 + \beta_5 + \beta_M = 1$, $0 \leq \beta_i \leq 1$.

Phase transformation from austenite to martensite is usually considered as non-diffusive transformation, which means that amount of volumetric phase is only a function of temperature (Chen *et al.*, 1997; Çetinel *et al.*, 2000; Reti *et al.*, 2001). This process may be described by the equation proposed by Koistinen and Marburger (1959),

$$\beta_M = \beta_A^0 \left[1 - e^{-k(M_s - T)}\right] \tag{1}$$

where β_A^0 is the amount of austenite at the beginning of transformation, k is a material property and T is the temperature. Under a stress-free state, M_s and M_f are the temperatures where martensitic transformation starts and finishes its formation. Assuming M_f as the temperature where martensitic phase reaches an amount of 99%, from Eq. (1), $k = 2\ln(10)/(M_s - M_f)$. In order to incorporate these limits in Eq. (1) and to assure the irreversibility of the martensite transformation, the following condition is defined (Hömberg, 1996):

$$\varsigma_{A \to M}\left(\dot{T}, T\right) = \Gamma\left(-\dot{T}\right)\Gamma\left(M_s - T\right)\Gamma\left(T - M_f\right) \tag{2}$$

where dot represent the differentiation with respect to time t and $\Gamma(x)$ is the Heaviside function (Hömberg, 1996; Chen *et al.*, 1997). The evolution of martensitic phase can be rewritten in a rate form as follows

$$\dot{\beta}_M\left(T, \dot{T}\right) = \varsigma_{A \to M}\, \beta_A^0 \left[\left(1 - \beta_M\right)\left(k\dot{T}\right)\right] \tag{3}$$

Pearlite, cementite, ferrite and bainite formations are usually considered as diffusion-controlled transformation, which means that they are time dependent. The evolution of these phase transformations can be predicted through an approximate solution using data from Time-Temperature-Transformation diagrams (*TTT*) (Çetinel *et al.*, 2000; Reti *et al.*, 2001). The analysis of phase transformation using this diagram is done considering that the cooling process may be represented by a curve divided in a sequence of isothermal steps, with a duration Δt, as shown in the Continuos-Cooling-Transformation diagram (*CCT*) of Fig. (1*a*). Through each isothermal step, the phase evolution is calculated considering isothermal transformation kinetics expressed by a *JMAK* law (Avrami, 1940; Cahn, 1956; Çetinel *et al.*, 2000; Reti *et al.*, 2001):

$$\beta_i(t) = \hat{\beta}_i^{\max}\left[1 - e^{-b_i\,(t)^{n_i}}\right] \qquad (i = 1, \ldots, 5) \tag{4}$$

Notice that β_i is the volumetric fraction of phase i, at a constant temperature T during the time t, measured from the start of cooling process; n_i is the Avrami exponent and b_i is a parameter that characterizes the rate of nucleation and growth processes (Avrami, 1940; Reti *et al.*, 2001). The parameter $\hat{\beta}_i^{\max}$ is represented by

$$\hat{\beta}_i^{\max} = \beta_i^{\max}\left[\sum_{j=1;\, j \neq i}^{5} \beta_j - \beta_M\right] \qquad (i = 1, \ldots, 5) \tag{5}$$

where $\beta_i^{\max}$ is a parameter that represents the maximum volumetric fraction for a phase i. These three parameters are function of temperature and can be obtained from *TTT* diagrams being usually presented in the form of curve fitted equations (Hömberg, 1996; Çetinel *et al.*, 2000; Reti *et al.*, 2001).

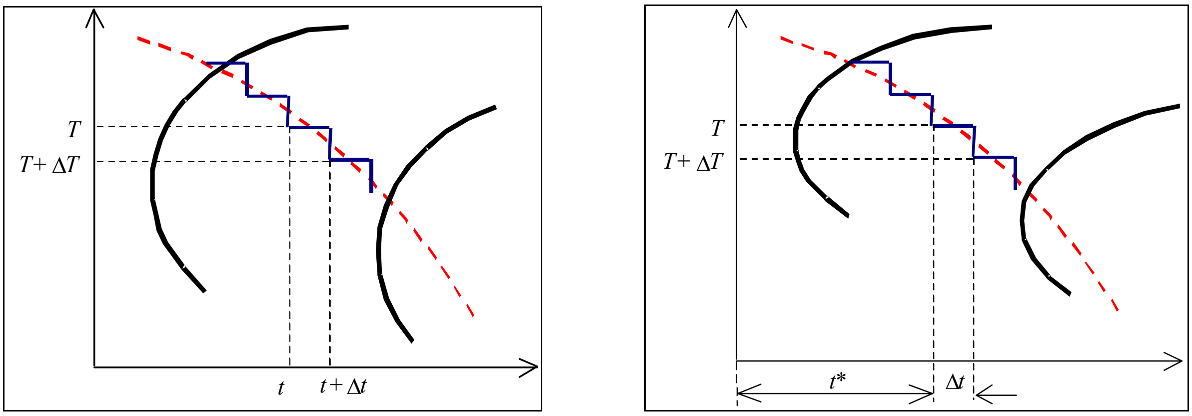

(*a*) (*b*)

Figure 1. (*a*) Cooling curve represented in a *CCT* diagram by a series of small isothermal time steps. (*b*) Fictitious time in the *TTT* diagram.

Equation (4) is valid for isothermal transformations and must be modified before it can be applied to the anisothermal process approximated by the sequence of isothermal steps shown in Fig. (1*a*). With this aim, a fictitious time t^* is defined to include effects associated with temperature change from step T to step $(T + \Delta T)$. The fictitious time t^* represents the time necessary for the formation of the volumetric fraction β_i at temperature T, considering an isothermal transformation developed at temperature $(T + \Delta T)$. This definition is considered as follows

$$t^* = \left[-\frac{1}{b_i(T+\Delta T)} \ln\left(1 - \frac{\beta_i(T)}{\hat{\beta}_i^{\max}(T+\Delta T))}\right)\right]^{\frac{1}{n_i(T+\Delta T)}} \qquad (i = 1, ..., 5) \tag{6}$$

This fictitious time is used as the starting point to compute the phase evolution during the isothermal time step Δt at temperature $(T + \Delta T)$, as shown in Fig.(1*b*). Now, the amount of volumetric phase at the end of the isothermal step $(T + \Delta T)$ at the time instant $(t + \Delta t)$ can be computed from (Çetinel *et al.*, 2000; Reti *et al.*, 2001):

$$\beta_i(T+\Delta T) = \hat{\beta}_i^{\max}(T+\Delta T)\left[1 - e^{-b_i(T+\Delta T)\,(t^*+\Delta t)^{n_i(T+\Delta T)}}\right] \qquad (i = 1, ..., 5) \tag{7}$$

The following condition must be defined to incorporate the temperature dependent functions, t_i^s and t_i^f that limits the beginning and the ending of the phase transformation, and also to assure its irreversibility

$$\varsigma_{A\to phase\,(i)}\left(\dot{T}, t\right) = \Gamma\left(-\dot{T}\right)\Gamma\left(t_i^f - t\right)\Gamma\left(t - t_i^s\right) \qquad (i = 1, ..., 5) \tag{8}$$

With these assumptions, the rate form of volumetric phase i is written as follows,

$$\dot{\beta}_i = \varsigma_{A\to phase\,(i)} \left\{ n_i (b_i)^{(1/n_i)} \left(\hat{\beta}_i^{\max} - \beta_i\right) \left[\ln\left(\frac{\hat{\beta}_i^{\max}}{\hat{\beta}_i^{\max} - \beta_i}\right)\right]^{\left(1 - \frac{1}{n_i}\right)} \right\} \qquad (i = 1, ..., 5) \tag{9}$$

3. Constitutive Model

Constitutive equations may be formulated within the framework of continuum mechanics and the thermodynamics of irreversible processes, by considering thermodynamic forces, defined from the Helmholtz free energy, ψ, and thermodynamic fluxes, defined from the pseudo-potential of dissipation, ϕ (Pacheco *et al.*, 2001).

The quenching model here proposed allows one to identify different coupling phenomena, estimating the effect of each one in the process. With this aim, a Helmholtz free energy is proposed as a function of observable variables, total strain, ε_{ij}, and temperature, T. Moreover, the following internal variables are considered: plastic strain, ε_{ij}^p, volumetric fractions of seven different microstructures, represented by phases in a macroscopic point of view, $\beta = (\beta_A, \beta_1, \beta_2, \beta_3, \beta_4, \beta_5, \beta_M)$. A variable related to kinematic hardening, α_{ij}, is also considered. Therefore, the following free energy is proposed, employing indicial notation where summation convention (i = 1,2,3) is evoked (Eringen, 1967), except when indicated:

$$\rho\psi(\varepsilon_{ij},\varepsilon_{ij}^{p},\alpha_{ij},\beta,T) = W(\varepsilon_{ij},\varepsilon_{ij}^{p},\alpha_{ij},\beta,T) = W_e(\varepsilon_{ij}-\varepsilon_{ij}^{p},\beta,T) + W_\alpha(\alpha_{ij}) + W_\beta(\beta) - W_T(T) \tag{10}$$

where ρ is the material density. The elastic strain is defined as follows:

$$\varepsilon_{ij}^{e} = \varepsilon_{ij} - \varepsilon_{ij}^{p} - \alpha_T(T-T_0)\delta_{ij} - \varepsilon_{ij}^{tv} - \varepsilon_{ij}^{tp} \tag{11}$$

In the right hand side of this expression, the first term is the total strain while the second is related to plastic strain. The third term is associated with thermal expansion. The parameter α_T is the coefficient of linear thermal expansion, T_0 is a reference temperature and δ_{ij} is the Kronecker delta. The fourth term is related to volumetric expansion associated with phase transformation from a parent phase $\varepsilon_{ij}^{tv} = (\sum_{r=1}^{6}\gamma_r\beta_r)\delta_{ij}$, where γ_r is a material phase property related to total expansion and $\beta_6 = \beta_M$. Finally, the last term is denoted as transformation plasticity strain $\dot{\varepsilon}_{ij}^{tp} = \sum_{r=1}^{6}\kappa_r\, g(\beta_r)\dot{\beta}_r\, \sigma_{ij}^{d}$, being the result of several physical mechanisms related to local plastic strain promoted by the phase transformation (Denis *et al.*, 1985; Sjöström, 1985; Desalos *et al.*, 1982); κ_r is a material phase parameter, $g(\beta_r)$ expresses the dependence on the transformation progress and σ_{ij}^{d} the deviatoric stress defined by $\sigma_{ij}^{d} = \sigma_{ij} - \delta_{ij}(\sigma_{kk}/3)$, with σ_{ij} being the stress tensor component. It should be emphasized that this strain may be related to stress states that are inside the yield surface. With these assumptions, energy functions may be expressed by,

$$\begin{aligned} W_e(\varepsilon_{ij}-\varepsilon_{ij}^{p},\beta_6,T) &= \Phi_{ijpq}E_{pqkl}\left[\tfrac{1}{2}\left(\varepsilon_{ij}-\varepsilon_{ij}^{p}\right)\left(\varepsilon_{kl}-\varepsilon_{kl}^{p}\right)-\left(\alpha_T\left(T-T_0\right)+\gamma_6\beta_6\right)\left(\varepsilon_{ij}-\varepsilon_{ij}^{p}\right)\delta_{kl}\right]+ \\ &+\frac{\Phi_{ijpq}E_{pqkk}\left[\tfrac{1}{2}\kappa_6\beta_6\left(2-\beta_6\right)\right]\Phi_{aaef}E_{efrs}\left[\tfrac{1}{2}\left(\varepsilon_{ij}-\varepsilon_{ij}^{p}\right)\left(\varepsilon_{rs}-\varepsilon_{rs}^{p}\right)-\left(\alpha_T\left(T-T_0\right)+\gamma_6\beta_6\right)\left(\varepsilon_{ij}-\varepsilon_{ij}^{p}\right)\delta_{rs}\right]}{\left(1-\Phi_{bbcd}E_{cdgg}\left[\tfrac{1}{2}\kappa_6\beta_6\left(2-\beta_6\right)\right]\right)} \end{aligned} \tag{12}$$

$$W_\alpha(\alpha_{ij}) = \frac{1}{2}H_{ijkl}\,\alpha_{ij}\alpha_{kl} \quad ; \quad W_\beta(\beta) = I_\beta(\beta) \quad ; \quad W_T(T) = \rho\int_{T_0}^{T} C_1\log(\xi)\,d\xi + \frac{\rho}{2}C_2\,T^2 \tag{13}$$

where $C_{ijpq} = \delta_{pi}\delta_{qj} + \frac{3}{2}E_{ijpq}\kappa_6\beta_6\left(2-\beta_6\right)$ and $\Phi_{ijpq} = C_{ijpq}^{-1}$. Tensor component Φ_{ijpq} is associated with the inverse of C_{ijpq} and $I_\beta(\beta)$ is the indicator function related to the convex set $C_\beta = \left\{\beta_i(i = A,1,2,3,4,5,6) \;|\; 0 \le \beta_i \le 1\right\}$ (Rockafellar, 1970).

Thermodynamics forces (σ_{ij}, P_{ij}, X_{ij}, $B^{\beta i}$, s), associated with state variables $(\varepsilon_{ij},\varepsilon_{ij}^{p},\alpha_{ij},\beta,T)$, are defined as follows:

$$\begin{aligned} \sigma_{ij} = \frac{\partial W}{\partial\varepsilon_{ij}} &= \Phi_{ijpq}E_{pqkl}\left[\varepsilon_{kl}-\varepsilon_{kl}^{p}-\left(\alpha_T\left(T-T_0\right)+\gamma_6\beta_6\right)\delta_{kl}\right]+ \\ &+\Phi_{ijpq}E_{pqkk}\left[\tfrac{1}{2}\kappa_6\beta_6\left(2-\beta_6\right)\right]\left\{\frac{\Phi_{aaef}E_{efrs}\left[\varepsilon_{rs}-\varepsilon_{rs}^{p}-\left(\alpha_T\left(T-T_0\right)+\gamma_6\beta_6\right)\delta_{rs}\right]}{1-\Phi_{bbcd}E_{cdgg}\left[\tfrac{1}{2}\kappa_6\beta_6\left(2-\beta_6\right)\right]}\right\} \end{aligned} \tag{14}$$

$$P_{ij} = -\frac{\partial W}{\partial\varepsilon_{ij}^{p}} = \sigma_{ij} \quad ; \quad X_{ij} = \frac{\partial W}{\partial\alpha_{ij}} = H_{ijkl}\alpha_{kl} \quad ; \quad s = -\frac{1}{\rho}\frac{\partial W}{\partial T} \tag{15}$$

$$B^{\beta_6} = \frac{\partial W}{\partial\beta_6} = -\left(\frac{\partial W_e}{\partial\beta_6}+Z_6\right) = E_{pqkl}\left(\varepsilon_{ij}-\varepsilon_{ij}^{p}\right)\left\{A_{ijpqkl}+\frac{E_{efrs}\delta_{kl}}{\Xi}\left[B_{ijpqefrs}+M_{ijpqefrs}+\frac{N_{ijpqefrs}}{\Xi}\right]\right\}-Z_6 \tag{16}$$

$$B^{\beta_i} = -\frac{\partial W}{\partial\beta_i} = -Z_i \qquad \text{for} \quad (i = 1, 2, 3, 4, 5) \tag{17}$$

where auxiliary tensors were defined:

$$\Xi = 1-\Phi_{zzhn}E_{hnxx}\left[\tfrac{1}{2}\kappa_6\beta_6\left(2-\beta_6\right)\right] \quad ; \quad \mathrm{A}_{ijpqkl} = \frac{\partial\Phi_{ijpq}}{\partial\beta_6}\left\{\left(\alpha_T\left(T-T_0\right)+\gamma_6\beta_6\right)\delta_{kl}-\tfrac{1}{2}\left(\varepsilon_{kl}-\varepsilon_{kl}^{p}\right)\right\}+\Phi_{ijpq}\gamma_6\delta_{kl} \tag{18}$$

$$\mathrm{B}_{ijpqefrs} = \left[\tfrac{1}{2}\kappa_6\beta_6(2-\beta_6)\right]\left(\frac{\partial\Phi_{ijpq}}{\partial\beta}\Phi_{aaef} + \Phi_{ijpq}\frac{\partial\Phi_{aaef}}{\partial\beta_6}\right)\left\{\left(\alpha_T(T-T_0)+\gamma_6\beta_6\right)\delta_{rs} - \tfrac{1}{2}\left(\varepsilon_{rs}-\varepsilon_{rs}^{p}\right)\right\} \tag{19}$$

$$\mathrm{M}_{ijpqefrs} = \Phi_{ijpq}\Phi_{aaef}\left\{\kappa_6(1-\beta_6)\left(\left(\alpha_T(T-T_0)+\gamma_6\beta_6\right)\delta_{rs} - \tfrac{1}{2}\left(\varepsilon_{rs}-\varepsilon_{rs}^{p}\right)\right) + \gamma_6\left[\tfrac{1}{2}\kappa_6\beta_6(2-\beta_6)\right]\delta_{rs}\right\} \tag{20}$$

$$\begin{aligned}\mathrm{N}_{ijpqefrs} = {} & \Phi_{ijpq}\left[\tfrac{1}{2}\kappa_6\beta_6(2-\beta_6)\right]\Phi_{aaef}\left\{E_{cdgg}\left(\frac{\partial\Phi_{bbcd}}{\partial\beta_6}\left[\tfrac{1}{2}\kappa_6\beta_6(2-\beta_6)\right] + \Phi_{bbcd}\kappa_6(1-\beta_6)\right)\right\} \\ & \left\{\left(\alpha_T(T-T_0)+\gamma_6\beta_6\right)\delta_{rs} - \tfrac{1}{2}\left(\varepsilon_{rs}-\varepsilon_{rs}^{p}\right)\right\}\end{aligned} \tag{21}$$

$Z_i \in \partial_\beta I_\beta(\beta)$ is the sub-differential of the indicator function I_β (Rockafellar, 1970).

In order to describe dissipation processes, it is necessary to introduce a potential of dissipation or its dual, which can be split into two parts: $\phi^*(P_{ij}, X_{ij}, B^\beta, g_i) = \phi_I^*(P_{ij}, X_{ij}, B^\beta) + \phi_T^*(g_i)$.

$$\begin{cases} \phi_{\mathrm{I}}^* = I_f^*(P_{ij}, X_{ij}) + \displaystyle\sum_{r=1}^{6} B^{\beta_r}\dot{\beta}_r \\ \phi_{\mathrm{T}}^* = \dfrac{T}{2}\Lambda\, g_i g_i \end{cases} \tag{22}$$

where $g_i = (1/T)\,\partial T/\partial x_i$ and Λ is the coefficient of thermal conductivity which is function of temperature; $I_f^*(P_{ij}, X_{ij})$ is the indicator function associated with elastic domain, related to the *von Mises* criterion (Lemaitre & Chaboche, 1990),

$$f(P_{ij}, X_{ij}) = \left[\tfrac{3}{2}(P_{ij}^d - X_{ij}^d)(P_{ij}^d - X_{ij}^d)\right]^{1/2} - \sigma_Y \le 0 \tag{23}$$

σ_Y is the material yield stress, $X_{ij}^d = X_{ij} - \delta_{ij}(X_{kk}/3)$ and $P_{ij}^d = \sigma_{ij}^d$.

With this assumption, thermodynamic fluxes, expressed as evolution laws obtained from ϕ^*, may be written as

$$\dot{\varepsilon}_{ij}^p \in \partial_{P_{ij}} I_f^*(P_{ij}, X_{ij}) = \lambda\,\mathrm{sign}\left(\sigma_{ij} - H_{ijkl}\alpha_{kl}\right) \quad ; \qquad \dot{\alpha}_{ij} \in -\partial_{X_{ij}} I_f^*(\sigma_{ij}, X_{ij}) = \dot{\varepsilon}_{ij}^p \tag{24}$$

$$\dot{\beta}_6 = \frac{\partial\phi^*}{\partial B^{\beta_6}} = \varsigma_{A\to M}\left[(1-\beta_6)k\dot{T}\right] \tag{25}$$

$$\dot{\beta}_i = \frac{\partial\phi^*}{\partial B^{\beta_i}} = \varsigma_{A\to phase\,(i)}\left\{n_i(b_i)^{(1/n_i)}\left(\beta_i^{\max} - \beta_i\right)\left[\ln\left(\frac{\beta_i^{\max}}{\beta_i^{\max}-\beta_i}\right)\right]^{\left(1-\frac{1}{n_i}\right)}\right\} \quad \text{for} \quad (i = 1, 2, 3, 4, 5) \tag{26}$$

$$q_i = -\frac{\partial\phi^*}{\partial g_i} = -\Lambda T\, g_i = -\Lambda\frac{\partial T}{\partial x_i} \tag{27}$$

where sign(x) = x / |x|, λ is the plastic multiplier from the classical theory of plasticity (Lemaitre & Chaboche, 1990) and q_i is the heat flux vector. Assuming that the specific heat is $c = -(T/\rho)\,\partial^2 W/\partial T^2$ and the set of constitutive Eqs. (14-17, 24-37), the energy equation can be written as (Pacheco, 1994):

$$\frac{\partial}{\partial x_i}\left(\Lambda\frac{\partial T}{\partial x_i}\right) - \rho c\dot{T} = -a_I - a_T \tag{28}$$

where

$$a_I = \sigma_{ij}\dot{\varepsilon}_{ij}^p - X_{\mathrm{ij}}\dot{\alpha}_{ij} + \sum_{r=1}^{6} + B^{\beta_r}\dot{\beta}_r \quad ; \quad a_T = T\left(\frac{\partial\sigma_{ij}}{\partial T}\left(\dot{\varepsilon}_{ij} - \dot{\varepsilon}_{ij}^p\right) + \frac{\partial X_{ij}}{\partial T}\dot{\alpha}_{ij} - \sum_{r=1}^{6}\frac{\partial B^{\beta_r}}{\partial T}\dot{\beta}_r\right) \tag{29}$$

Terms a_I and a_T are, respectively, internal and thermal coupling. In this article, both terms are neglected and thermal problem is solved as a rigid body.

4. Cylindrical Bodies

This contribution considers cylindrical bodies as an application of the proposed general formulation. Other references present different analyses of this problem (Pacheco *et al.*, 1997; Camarão *et al.*, 2000; Silva *et al.* 2002). With this assumption, heat transfer analysis may be reduced to a one-dimensional problem. Also, plane stress or plane strain state can be assumed. Under these assumptions, only radial, r, circumferential, θ, and longitudinal, z, components need to be considered and a one-dimensional model is formulated. For this case, tensor quantities presented in previous section may be replaced by scalar or vector quantities. As examples, one could mention: E_{ijkl} replaced by E; H_{ijkl} replaced by H; σ_{ij} replaced by σ_i (σ_r , σ_θ , σ_z). A detailed description of these simplifications could be found in Pacheco *et al.* (2001*a*).

The numerical procedure here proposed is based on the operator split technique (Ortiz *et al.*, 1983; Pacheco, 1994) associated with an iterative numerical scheme in order to deal with non-linearities in the formulation. With this assumption, coupled governing equations are solved from four uncoupled problems: thermal, phase transformation, thermo-elastic and elastoplastic.

Thermal Problem - Comprises a radial conduction problem with convection. Material properties depend on temperature, and therefore, the problem is governed by non-linear parabolic equations. An implicit finite difference predictor-corrector procedure is used for numerical solution (Ames, 1992; Pacheco, 1994).

Phase Transformation Problem – The volumetric fractions of the phases are determined in this problem. Evolution equations are integrated from a simple implicit Euler method (Ames, 1992; Nakamura, 1993).

Thermo-elastic Problem - Stress and displacement fields are evaluated from temperature distribution. Numerical solution is obtained employing a shooting method procedure (Ames, 1992; Nakamura, 1993).

Elastoplastic Problem - Stress and strain fields are determined considering the plastic strain evolution in the process. Numerical solution is based on the classical return mapping algorithm (Simo & Miehe, 1992; Simo & Hughes, 1998).

5. Numerical Simulations

As an application of the general proposed model, numerical investigations associated with the quenching of long steel cylindrical bar of SAE 4140H steel with radius R are carried out. Numerical simulations include progressive induction hardening (PIH) and through hardening (TH). PIH is a heat treatment process carried out by moving a workpiece at a constant speed through a coil and a cooling ring. Applying an alternating current to the coil, a magnetic field is generated inducing eddy currents that heats the workpiece and promotes the formation of a thin surface layer of austenite. Afterwards, a cooling fluid is sprayed on the surface by the cooling ring promoting the quenching of the layer, which is transformed into martensite, pearlite, bainite and proeutectoid ferrite/cementite depending on, among other things, the cooling rate. A hard surface layer with high compressive residual stresses, combined with a tough core with tensile residual stresses, is often obtained. TH consists of heating the steel, usually in a furnace, to a suitable austenitizing temperature, holding at that temperature for a sufficient time to effect the desired change in crystalline structure, and immersing and cooling in a suitable liquid medium.

Material parameters of the cylinder are the following (Denis *et al.*, 1985; Denis *et al.*, 1999; Woodard, *et al.*, 1999; Sjöström, 1985; Melander, 1985; Leblond *et al.*, 1989): $\gamma_1 = 3.333\text{x}10^{-3}$, $\gamma_2 = 0$, $\gamma_3 = \gamma_4 = \gamma_5 = 5.000\text{x}10^{-3}$, $\gamma_6 = 1.110 \text{ x } 10^{-2}$, $\kappa_i = (5/(2\sigma_y^A))\gamma_i$ (where σ_y^A is the austenite yielding stress and $i = 1,2,3,4,5,6$), $\rho = 7.800 \text{ x } 10^3$ Kg/m^3, $M_s = 370$ °C, $M_f = 260$ °C. Other parameters depend on temperature and needs to be interpolated from experimental data. Therefore, parameters E, H, σ_Y, α_T, c, Λ and the convection coefficient, h, are evaluated by polynomial expressions (Melander, 1985; Hildenwall, 1979; Pacheco *et al.*, 2001*a*; Silva *et al.*, 2002). Temperature dependent parameters for diffusive phase transformations presented in Section 2 were obtained from *TTT* diagrams (ASM, 1977).

After a convergence analysis, a spatial discretization of 81 points was adopted for the numerical simulations.

At first, the proposed multi-phase model is employed in order to analyze the phase products for simple cooling curves. Figure (2*a*) shows a *TTT* diagram for SAE 4140H steel where points represent experimental data (ASM, 1977) while lines represents fitted curves. Figure (2*b*) shows a *CCT* diagram for the same steel (ASM, 1977) where colored lines 1 to 5 represent five different cooling curves obtained from data fitting and used as temperature evolution input for the multi-phase model. Table (1) presents a comparison between values predicted by the model and experimental data obtained from this *CCT* diagram. Errors smaller than 16% were observed in the transformed volumetric phase fractions at the end of cooling. These results may be considered as good predictor since experimental data has a large dispersion.

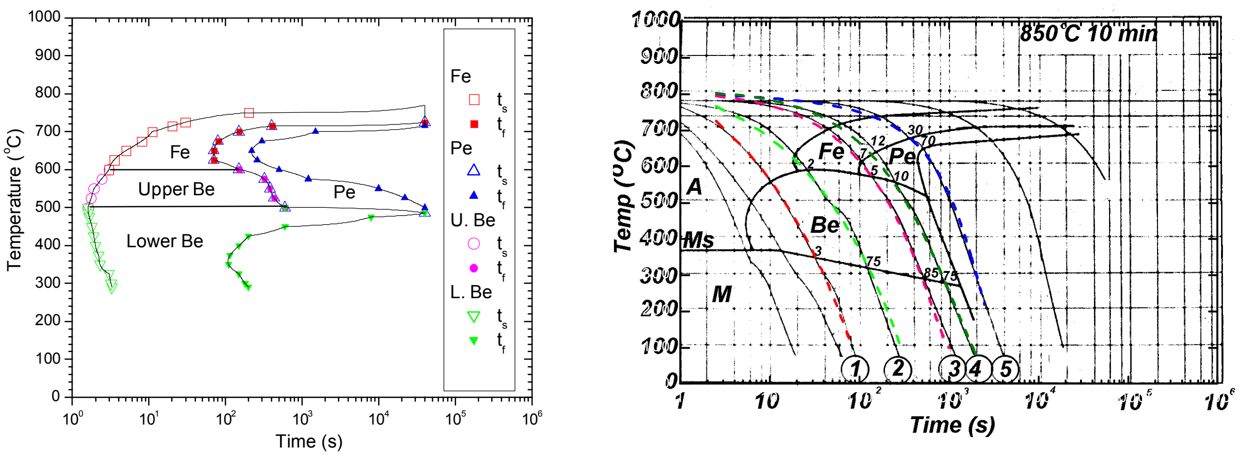

(*a*) (*b*)

Figure 2. SAE 4140H. (*a*) *TTT* diagram with fitted parameters t_i^s and t_i^f . (*b*) Five cooling curves in a *CCT* diagram.

Table 1. Predicted values and experimental data obtained from a *CCT* diagram for SAE 4140H.

	Cooling Curve 1		Cooling Curve 2		Cooling Curve 3		Cooling Curve 4		Cooling Curve 5	
	CCT	Predicted	*CCT*	Predicted	*CCT*	Predicted	*CCT*	Predicted	*CCT*	Predicted
Bainite	3	14	75	60	85	84	75	63	0	0
Ferrite	0	0	2	1	7	12	12	19	30	33
Perlite	0	0	0	0	5	4	10	18	70	67
Martensite	97	86	23	39	3	0	3	0	0	0

PIH simulations regards a cylinder with a radius R = 22.5 mm, where a 3 mm thickness layer is heated to 850°C for 10s and then, immersing in a liquid medium at 20°C until time instant 120s is reached. Experimental results for PIH in cylindrical bodies, discussed in Camarão (1998) and Pacheco *et al.* (2001*a*, 2001*b*) are used as reference for the comparison with numerical results here obtained. Experimental results, obtained for similar conditions, furnish circumferential (σ_θ) and longitudinal (σ_z) residual stress values at the surface of –830 MPa and –500 MPa, respectively. These values, measured through X-ray diffraction technique, present an uncertainty of 30 MPa. Moreover, hardness measurements and metallographic analysis are performed to identify the martensitic hardened layer.

Temperature time history for different positions of the cross-section is presented in Fig. (3a). Notice that for layers deeper than 3 mm, temperature does not reach austenitizing limit.

The stress distribution over the radius for the final time instant is presented in Fig. (3b). Notice the stress values on the external surface, $\sigma_\theta = -879$ MPa and $\sigma_z = -274$ MPa. The circumferential stress, σ_θ, is close to experimental results. The longitudinal stress, σ_z, on the other hand, presents a discrepancy that could be explained by the assumption of plane strain state adopted to simulate the restriction associated with adjacent regions of the heated region, which is at lower temperatures.

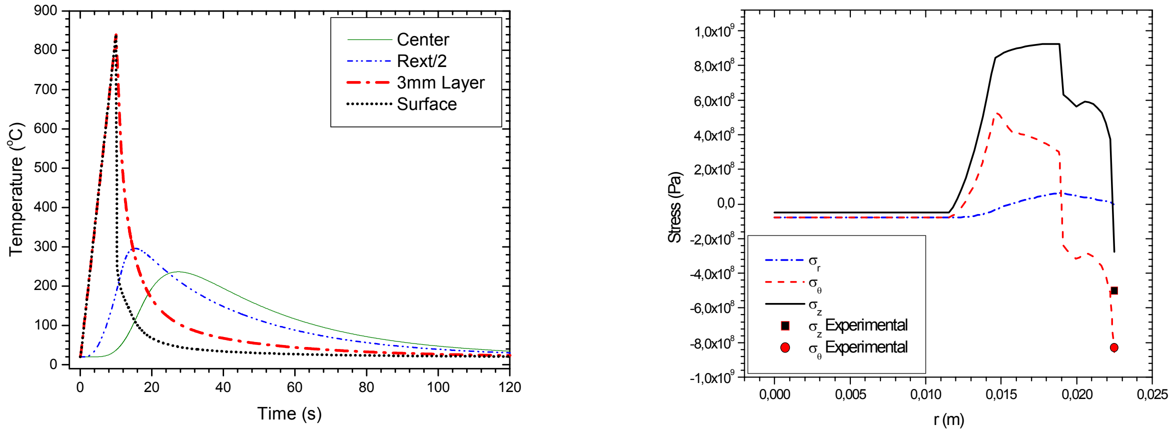

(a) (b)

Figure 3. PIH quenched cylinder (R = 22.5 mm): (*a*) Temperature time history for different positions and (*b*) stress distribution for final time instant.

Figures (4a) and (4b) show PIH experimental measures (Camarão, 1998). Figure (4a) shows a cross-section of a quenched bar submitted to a Nital 2% etch, while Fig. (4b) presents its hardness measures. In order to compare numerical and experimental results, a relation between volume fraction of phases and hardness is established.

Therefore, it is assumed that martensitic phase (β_6) has 60 HR$_C$ while a value of 30 HR$_C$ is adopted for the regions where martensitic phase is not present, that is, this value is considered as a mean value of hardness among the other phases. Figure (4c) presents the martensite volumetric fraction distribution for final time instant. The process quenches only points from external surface to 3 mm deep. Outside this region, retained austenite is observed. Once again, numerical results predicted by the model are closer to experimental data.

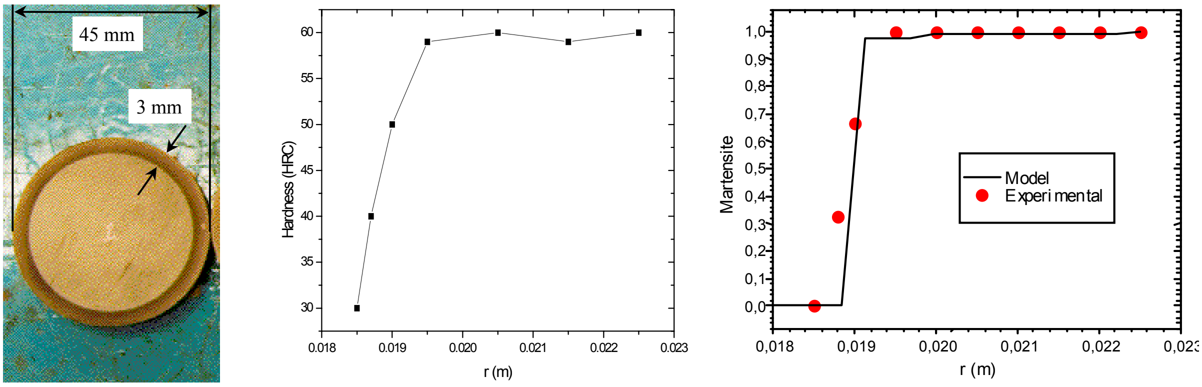

(a) (b) (c)

Figure 4. PIH quenched cylinder (R = 22.5 mm): (a) Cross-section view (Nital 2% etch), (b) hardness measures and (c) and martensite volumetric fraction distribution for final time instant.

A less severe cooling condition is now considered for TH simulations. Therefore TH simulations concerns a cylinder with R = 38.1 mm heated to an homogeneous temperature of 850°C which is immersed in mineral oil Durixol V35 at 60°C until time instant 1200 s (≅ 20 min) is reached. Since all cylinder sections experiment the same thermal history and the longitudinal direction is free, a plane stress state is adopted. As in the previous case, the convection coefficient, h, is temperature dependent and it is interpolated from experimental data presented by Ma (2002) and reproduced in Fig. (5a). Temperature time history for different positions of the cross-section is presented in Fig. (5b) in a time log scale. The highly non-linear temperature dependence of the thermal parameters, especially h, promotes a complex temperature evolution where the cooling rate varies considerably.

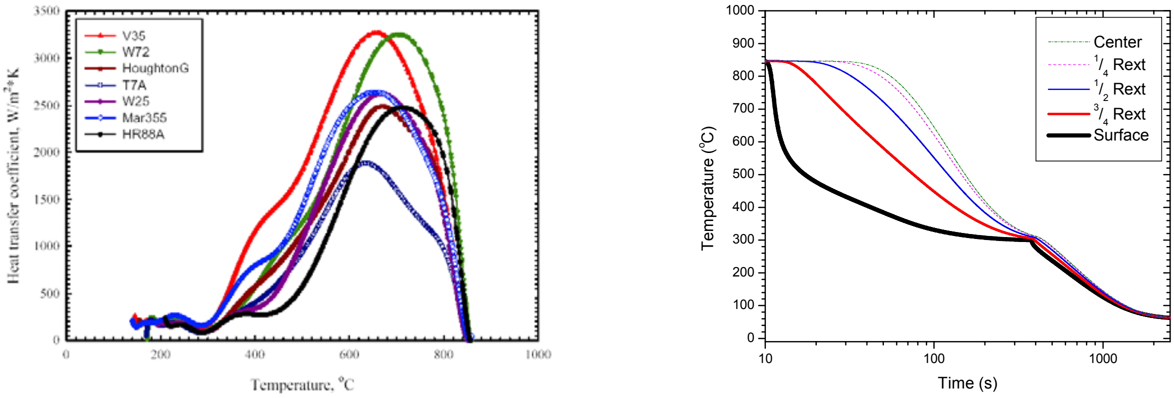

(a) (b)

Figure 5. TH quenched cylinder (R = 38.1 mm): (*a*) Convection coefficient, h, for mineral oils (Ma, 2002) and (*b*) temperature time history for different positions.

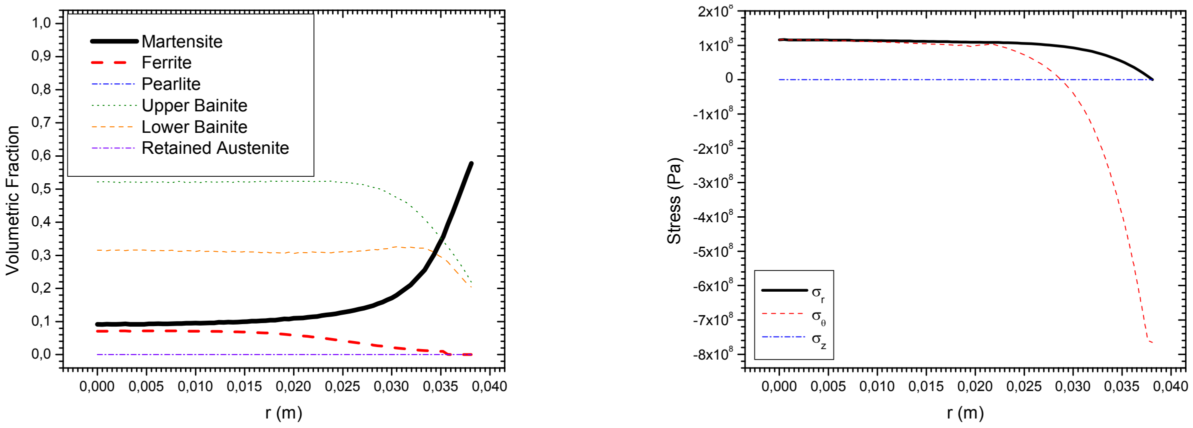

(a) (b)

Figure 6. TH quenched cylinder (R = 38.1 mm): (*a*) phase and (*b*) stress distributions for the final time instant.

Values of volumetric fractions of each phase and stress distributed through the radius of the cylinder are shown in Fig. (6) for the final time instant. Compressive circumferential stress is noted at the surface of the cylinder. This simulation shows important information that could be furnished by the model since the presence of tensile residual stresses at the cylinder surface can be especially dangerous for mechanical purposes. Notice that tensile stress fields normally initiate fatigue cracks. Therefore, the prediction of such stresses allows the development of more precise methodologies for assessing the structural integrity of mechanical components. Figure (7) shows the volumetric fraction time evolution of the microstructural phases at the center and at the surface.

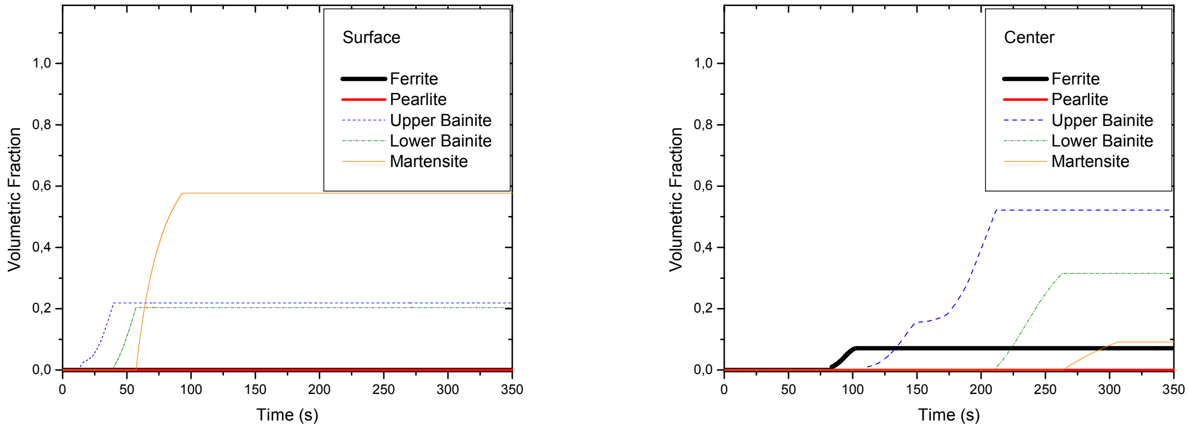

(a) (b)

Figure 7. TH quenched cylinder (R = 38.1 mm): Volumetric fraction phase evolution at center (a) and surface (b).

6. Conclusions

The present contribution regards on modeling and simulation of quenching process, presenting an anisothermal multi-phase constitutive model formulated within the framework of continuum mechanics and thermodynamics of irreversible processes. This approach allows a direct extension to more complex situations, as the analysis of three-dimensional media. A numerical procedure is developed based on the operator split technique associated with an iterative numerical scheme in order to deal with non-linearities in the formulation. The proposed numerical procedure allows the use of traditional numerical methods, like the finite element method. Progressive induction hardening and through hardening of cylindrical bodies are considered as applications of the proposed general formulation. Numerical results show that the proposed model is capable of capturing the general behavior of experimental data. Therefore, it can be used as a powerful tool to predict the thermomechanical behavior of quenched mechanical components and choose important parameters as the cooling medium and the induced layer thickness.

7. Acknowledgements

The authors would like to acknowledge the support of the Brazilian Research Agencies CNPq and CAPES.

8. References

Ames, W.F., 1992, "*Numerical Methods for Partial Differential Equations*", Academic Press.

ASM, 1977, *"Atlas of Isothermal Transformation and Cooling Transformation Diagrams"*, American Society Metals.

Avrami, M., 1940, "Kinetics of Phase Change. II: Transformation-Time relations for random distribution of nuclei", *Journal of Chem. Phys.*, v.8, pp.212.

Cahn, J.W., 1956, "Transformation Kinetics During Continuous Cooling", *Acta Metallurgica*, v.4, pp.572-575.

Camarão, A.F., 1998, "A Model to Predict Residual Stresses in the Progressive Induced Quenching of Steel Cylinders", Ph.D. Thesis, Department of Metallurgical and Materials Engineering - USP, in Portuguese.

Camarão, A.F., da Silva, P.S.C.P. and Pacheco, P.M.C.L., 2000, "Finite Element Modeling of Thermal and Residual Stresses Induced by Steel Quenching", *Seminário de Fratura, Desgaste e Fadiga de Componentes Automobilísticos*, Brazilian Society of Automotive Engineering, in Portuguese.

Çetinel, H., Toparlı, M. & ÖZsoyller, 2000, "A Finite Element Based Prediction of the Microstructural Evolution of Steels Subjected to the Tempcore Process", *Mechanics of Materials*, 32, pp.339-347.

Chen, J.R., Tao, Y.Q. & Wang, H.G., 1997, "A Study on Heat Conduction with Variable Phase Transformation Composition during Quench Hardening", *Journal of Materials Processing Technology*, 63, pp.554-558.

Denis, S., Gautier, E., Simon, A. and Beck, G., 1985, "Stress-Phase-Transformation Interactions – Basic Principles, Modelling and Calculation of Internal Stresses", *Material Science and Technology*, v.1, October, p.805-814.

Denis, S., Sjöström, S. & Simon, A., 1987, "Coupled Temperature, Stress, Phase Transformation Calculation Model Numerical Illustration of the Internal Stresses Evolution during Cooling of a Eutectoid Carbon Steel Cylinder", *Metallurgical Transactions A*, v. 18A, July, pp.1203-1212.

Denis, S., Farias, D. & Simon, A., 1992, “Mathematical Model Coupling Phase Transformation and Temperature Evolutions in Steels”, *ISIJ International*, v.32, No. 3, pp.316-326.

Denis S., 1996, “Considering Stress-Phase Transformation Interaction in the Calculation of Heat Treatment Residual Stresses”, Journal de Physique IV, v.6, January, pp.159-174.

Denis, S., Archambault, S., Aubry, C., Mey, A., Louin, J.C. and Simon, A., 1999, “Modelling of Phase Transformation Kinetics in Steels and Coupling with Heat Treatment Residual Stress Predictions”, *Journal de Physique IV*, v.9, September, pp.323-332.

Desalos, Y., Giusti, J. and Gunsberg, F., 1982, “Deformations et Contraintes lors du Traitment Thermique de Pieces de Acier”, *RE902, Institut de Recherches de la Sidérugie Française*.

Eringen, A.C., 1967, “*Mechanics of Continua*”, John Wiley, New York.

Fernandes, M. B., Denis, S. & Simon, A., 1985, “Mathematical Model Coupling Phase Transformation and Temperature Evolution during Quenching of Steels”, Materials Science and Technology, v.1, October, pp.838-844.

Gür, C.H. & Tekkaya, A.E., 1996, “Finite Element Simulation of Quench Hardening”, *Steel Research*, Vol.67, No.7, pp.298-306.

Gür, C.H., Tekkaya, A.E. & Schuler,W., 1996, “Effect of Boundary Conditions and Workpiece Geometry on Residual Stresses and Microstructure in Quenching Process”, *Steel Research*, Vol.67, No.11, pp.501-506.

Gür, C.H. & Tekkaya, A.E., 2001, “Numerical Investigation of Non-Homogeneous Plastic Deformation in Quenching Process”, *Materials Science and Engineering*, A319-321, pp.164-169.

Inoue, T. & Wang, Z., 1985, “Coupling between Stress, Temperature, and Metallic Structures during Processes Involving Phase Transformations”, Material Science and Technology, Vol.1, pp.845-850.

Hildenwall, B., 1979, “*Prediction of the Residual Stresses Created During Quenching*”, Ph.D. Thesis, Linkoping Univ.

Hömberg, D., 1996, “A Numerical Simulation of the Jominy End-quench Test”, Acta Mater., v.44, n.11, pp.4375-4385.

Koistinen, D.P. and Marburger, R.E., 1959, “A General Equation Prescribing the Extent of the Austenite-Martensite Transformation In Pure Iron-Carbon Alloys and Plain Carbon Steels”, *Acta Metallurgica*, v.7, pp.59-60.

Leblond, J.B. and Devaux, J. and J.C. Devaux, 1989, “Mathematical Modelling of Transformation Plasticity in Steels - I: Case of Ideal-Plastic Phases”, *International Journal of Plasticity*, Vol. 5, pp.551-572.

Lemaitre, J. and Chaboche, J.-L., 1990, “*Mechanics of Solid Materials*”, Cambridge Press.

Ma, S., 2002, “Characterization of the Performance of Mineral Oil based Quenchants using CHTE Quench Probe System”, M.Sc. Thesis, Department of Materials Science and Engineering, Worcester Polytechnic Institute.

Melander, M., 1985, “*A Computational and Experimental Investigation of Induction and Laser Hardening*”, Ph.D. Thesis, Department of Mechanical Engineering, Linkoping University.

Nakamura, S., 1993, “*Applied Numerical Methods in C”*, Prentice-Hall.

Ortiz, M., Pinsky, P.M. and Taylor, R.L., 1983, “Operator Split Methods for the Numerical Solution of the Elastoplastic Dynamic Problem”, *Computer Methods in Applied Mechanics and Engineering*, v.39, pp.137-157.

Pacheco, P.M.C.L., 1994, “*Analysis of the Thermomechanical Coupling in Elasto- Viscoplastic Materials*”, Ph.D. Thesis, Department of Mechanical Engineering, PUC-Rio, in Portuguese.

Pacheco, P.M.C.L., Oliveira, S.A., Camarão, A.F. and Savi, M.A., 1997, “A Model to Predict Residual Stresses Introduced by the Quenching Process in Steels”, *In Proceedings of the COBEM 97 - XIV Brazilian Congress of Mechanical Engineering – ABCM* (in Portuguese).

Pacheco, P.M.C.L., Savi, M.A. & Camarão A.F., 2001a, “Analysis of Residual Stresses Generated by Progressive Induction Hardening of Steel Cylinders”, *Journal of Strain Analysis for Engineering Design*, v.36, n.5, pp.507-516.

Pacheco, P.M.C.L., Savi, M.A. & Camarão, A.F., 2001b, “Quenching Generated Residual Stresses in Steel Cylinders”, *In Proceedings of the XV Brazilian Congress of Mechanical Engineering – ABCM*, November 22-26, Águas de Lindóia, Brazil (in Portuguese).

Reti, T., Fried, Z. & Felde, I., 2001, “Computer Simulation of Steel Quenching Process using a Multi-Phase Transformation Model”, *Computational Materials Science*, 22, pp. 261-278.

Rockafellar, R.T., 1970, “*Convex Analysis*”, Princeton Press.

Sen, S., Aksakal, B. and Ozel, A., 2000, “Transient and Residual Thermal Stresses in Quenched Cylindrical Bodies”, *International Journal of Mechanical Sciences*, v.42 n.10, p.2013-2029.

Silva, E.P., Pacheco, P.M.C.L. & Savi, M.A., 2002, “On the Thermo-Mechanical Coupling in Austenite-Martensite Phase Transformation Related to The Quenching Process”, submitted to the *International Journal of Solids and Structures*.

Simo, J.C. and Miehe, C., 1992, “Associative Coupled Thermoplasticity at Finite Strains: Formulation, Numerical Analysis and Implementation”, *Computer Methods in Applied Mechanics and Engineering*, v.98, pp.41-104.

Simo, J.C. and Hughes, T.J.R., 1998, “Computational Inelasticity”, Springer.

Sjöström, S., 1985, “Interactions and Constitutive Models for Calculating Quench Stresses in Steel”, *Material Science and Technology*, v.1, p.823-829.

Sjöström, S., 1994, “Physical, Mathematical and Numerical Modelling for Calculation of Residual Stresses: Fundamentals and Applications”, *In Proceedings of the Fourth International Conference on Residual Stresses*, June 8-10, Baltimore, USA.

Woodard, P.R., Chandrasekar, S., Yang, H.T.Y., 1999, “Analysis of Temperature and Microstructure in the Quenching of Steel Cylinders”, *Metallurgical and Materials Transactions B-Process Metallurgy and Materials Processing Science*, v.4, August, p.815-822.